buildings

MDPI

Article

Optimizing Indoor Microclimate and Thermal Comfort Through Sorptive Active Elements: Stabilizing Humidity for Healthier Living Spaces

Jitka Peterková [1,*], Jiří Zach [1], Vítězslav Novák [1], Azra Korjenic [2], Abdulah Sulejmanovski [2] and Eldira Sesto [2]

[1] Institute of Technology of Building Materials and Components, Faculty of Civil Engineering, Brno University of Technology, Veveri 331/95, 602 00 Brno, Czech Republic; jiri.zach@vut.cz (J.Z.); vitezslav.novak1@vut.cz (V.N.)

[2] Vienna Institute of Material Technology, Building Physics and Building Ecology, Faculty of Civil Engineering, TU Wien, Karlsplatz 13, 1040 Vienna, Austria; azra.korjenic@tuwien.ac.at (A.K.); abdulah.sulejmanovski@tuwien.ac.at (A.S.); eldira.sesto@tuwien.ac.at (E.S.)

* Correspondence: jitka.peterkova@vut.cz; Tel.: +420-(54)-1147524

Abstract: This paper investigates the potential use of natural materials and elements for stabilizing indoor humidity levels, focusing on creating healthier living environments in buildings. Unstable indoor microclimates, particularly extreme humidity levels, can negatively affect human health by causing issues such as condensation, mold growth, or dry mucous membranes. In this work, we explore how sorptive materials can maintain indoor humidity within the optimal range of 40–50%. The aim is to identify optimal solutions for moisture control using passive elements, such as unfired ceramic components, which demonstrate high sorption activity within the 35–55% relative humidity range. These elements can effectively absorb moisture from, or release it back into, the indoor environment as needed. Five clay types based on different clay minerals were analyzed in the research in order to assess how their structures influence moisture adsorption behavior. These elements can be combined with green/active elements and standard measures, such as ventilation or targeted room air exchange, to improve indoor humidity regulation. The evaluation of the results so far indicates that the use of clay-based elements in the interior offers a sustainable and natural approach to maintaining optimal indoor microclimate conditions. The slab elements from all 5 clay formulations investigated effectively support indoor humidity stabilization.

Keywords: non-fired ceramic; clay minerals; microclimate; sorption/desorption of moisture; moisture buffering capacity; internal environment of buildings

Citation: Peterková, J.; Zach, J.; Novák, V.; Korjenic, A.; Sulejmanovski, A.; Sesto, E. Optimizing Indoor Microclimate and Thermal Comfort Through Sorptive Active Elements: Stabilizing Humidity for Healthier Living Spaces. *Buildings* **2024**, *14*, 3836. https://doi.org/10.3390/buildings14123836

Academic Editor: Jiying Liu

Received: 8 October 2024
Revised: 31 October 2024
Accepted: 7 November 2024
Published: 29 November 2024

1. Introduction

Unsuitable indoor environments pose a significant problem not only for the building itself but also for the health of its occupants. Background pollutants are a group of pollutants in the indoor environment that act continuously and diffuse freely into the space. These include both substances produced by humans (water vapor, CO_2) and substances released from materials, furnishings, and products used in the living space (e.g., formaldehyde, VOCs). These pollutants can result in different conditions, such as condensation, mold growth, and mites, which can lead to health issues ranging from fatigue and dizziness to major health complications. Healthy building environments can be effectively influenced by proper design and composition of the building structure (including materials used), optimization of airflow and ventilation [1,2], green elements and green facades, or by using sorptive active materials [3,4]. This is how you can ensure the thermal comfort of buildings, which is influenced by both subjective factors depending on the characteristics of people and objective factors, which include air temperature, reactive air humidity, airflow speed, and the temperature of surrounding walls or objects. It is generally known that relative

humidity affects thermal comfort, and humidity itself also affects the properties of the materials used [5,6]. In addition to the physical parameters of the environment, there are also analytical methods for predicting the ergonomics of the indoor environment. One of them is the PMV index (prediction of mean thermal sensation), which indicates the average value of the choice of numerous groups of people classified on a temperature scale. It is based on the thermal balance of human heat and the environment, where a balance is sought between the internal production of human heat and its loss to the environment as part of wet sweating in a warmer environment. From the environmental point of view, air temperature and mean radiation temperature, relative air humidity, and flow speed are included in the calculation. In addition to environmental parameters, the calculation also includes the level of metabolic heat production depending on the type of work and the insulation that is provided by clothing, according to the EN ISO 7730 standard [7]. The PMV index shows the average choice of perception of the environment of a large group of people; individual feelings may be different. For this reason, the PPD index (predicted percentage dissatisfied) has been introduced, which expresses the number of people who will be dissatisfied with the state of the environment. The index expresses the percentage of people who will feel hot or cold and will be dissatisfied with the state of the environment [7].

Interior humidity can be effectively regulated by ventilation (both natural and forced), by special HVAC air treatment devices, and by sorption-active elements, which, thanks to an efficient capillary system, allow the sorption and transport of moisture and water vapor. For these materials in the building market today, waste materials are often used with binders and other additives or natural materials (e.g., calcium silicate Ca_2SiO_3 plates, coniferous wood, etc.). Clay plasters, which have been used extensively throughout history, also work very well in terms of interior moisture control. This natural material creates a healthy indoor microclimate by effectively managing indoor humidity levels. This issue is being addressed by a number of experts worldwide who are conducting detailed research into different types of clay plasters, including the possible use of abrasives, binders, reinforcing fibers, etc. McGregor et al. presented the results of research where they found that unfired clay elements have a significant ability to regulate indoor humidity compared to conventional building materials [8]. Experts from China, Yao et al., have investigated the thermal and hygric behavior of clay/sand composites in 70:30 and 30:70 ratios and found that the clay/sand ratio has less influence on thermal properties compared to hygric properties. The vapor permeability coefficient and equilibrium moisture content are relatively higher in samples with lower sand content, and this difference increases under high humidity conditions compared to samples with higher sand content. The permeability of samples with higher sand content is also relatively higher. The clay/sand ratio significantly affects the variation in moisture content of earthen plasters. Under high humidity conditions, the difference in moisture content between the two types becomes more significant [9]. Emiroğlu et al. determined that the optimal mixing ratios for raw materials in ready-mixed clay plasters (clay and sand) range from 0.43 to 0.66 by weight [10]. Palumbo et al. investigated the effect of natural fillers on the hygrothermal properties of clay plasters. They concluded that the addition of vegetable materials in earth mixtures has much more impact on the density and the thermal conductivity of the materials than on their water vapor permeability and moisture buffering capacity. Mixtures incorporating highly porous vegetable materials such as corn pith might be more appropriate for indoor environments with short and intense moisture loads [11].

Scientists at the St. Petersburg State Institute of Technology developed mineral-carbon composite sorption-active materials based on man-made waste, using pyrolyzed used tires as a filler and montmorillonite-rich bentonite clay from excavations as a binder [12]. A number of studies examined the moisture behavior of clay-based composite finishes, including their effect on a healthy indoor microclimate. For example, Deliniere et al. [13] describe clay plasters as interior moisture regulators suitable for both new buildings and historical renovations. Darling et al. [14] describe clay materials as passive removal ma-

terials that effectively control indoor pollution without substantial formation of chemical byproducts and without an energy penalty. Clay plasters can improve perceived air quality by significantly reducing both ozone and aldehyde concentrations, which adversely affect human health. Madison et al. [15] tested clay-sand plasters reinforced with wool fibers from *Typha* spadixes and chips of *Typha* and *Phragmites*, evaluating their ability to balance indoor air humidity through absorption and desorption. It was found that the natural fibers of the sedge (*Typha latifolia*) had a positive effect on the water absorption and desorption of these organic materials. Liuzzi et al. [16] investigated the thermal and humidity behavior of lime-stabilized clay composites, including quarry fine, kaolinite, and bentonite. Results demonstrated that the earth-bentonite gave the best hygric performance in terms of humidity buffering and, when combined with an HVAC system, achieved a significant 30% operational energy saving in humidification and dehumidification. Other experts dealing with eco-friendly natural fiber composites and their humidity behavior are Zhou et al. [17], Abbas et al. [18], Gentile et al. [19], Mazhoud et al. [20], and He et al. [21,22]. Based on the results of many scientific works and theoretical knowledge, it can be concluded that clay-based plaster can effectively balance indoor air humidity throughout the year by absorbing and releasing moisture. However, it must be noted that the specific composition, particularly the clay mineral content, is crucial for optimal performance. The moisture behavior is influenced by the type and structure of clay minerals. Kaolinite ($Al_2O_3 \cdot 2SiO_2 \cdot 2H_2O$) is classified as a double-layered mineral in which layers of Si-O tetrahedra and Al-(OH) octahedra alternate regularly in the lattice. These layers are strongly attracted to each other. The thickness of the bilayer is 0.7 nm, including the interlayer at 0.715 nm. On the other hand, the minerals montmorillonite ($Al_2O_3 \cdot 4SiO_2 \cdot nH_2O$) and illite ($nK_2O \cdot Al_2O_3 \cdot 3SiO_2 \cdot nH_2O$) are trilayer minerals, where in their lattice there is a layer of Al-(OH) octahedra between two layers of Si-O tetrahedra. Since the trilayers are always facing each other with layers of Si-O tetrahedra, there is less attraction between them, i.e., water can enter these spaces more easily. In the case of montmorillonite, the layer thickness is 0.95 nm, and cations (e.g., Ca^{2+}, Na^{+}, Mg^{2+}) are absorbed between the trilayers surrounded by layers of water, thus increasing the distance between the trilayers to an average of 1.4 nm. In the case of illite, the silicon ions in the tetrahedra are replaced by aluminum ions up to 20%, and the thickness of the trilayers is 1 nm. The crystal lattices of the individual minerals are shown in the following Figure 1 [23–25].

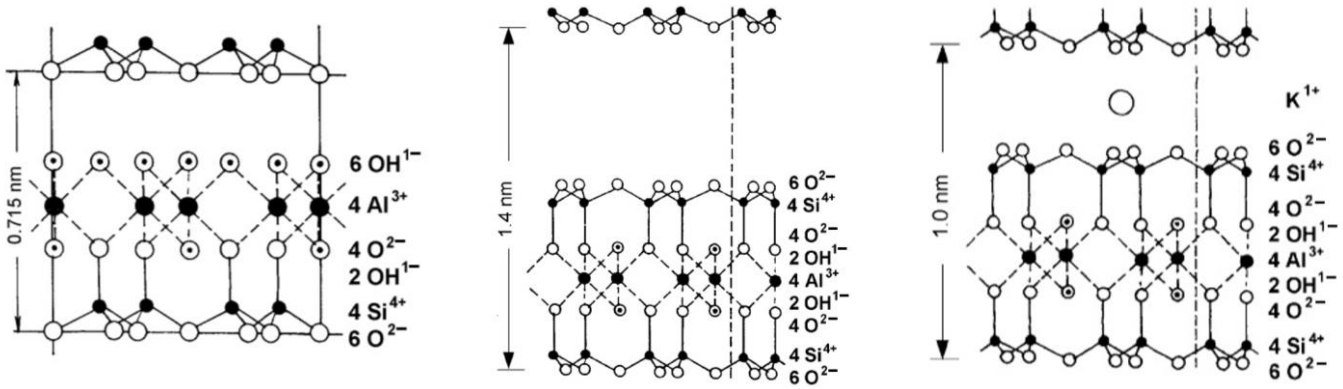

(**a**) (**b**) (**c**)

Figure 1. Grid of individual clay minerals. (**a**) Kaolinite, (**b**) montmorillonite, and (**c**) illite.

This paper's findings reveal the possible use of natural materials and their elements to stabilize indoor humidity in building environments.

The research, carried out in cooperation between the Faculty of Civil Engineering at Brno University of Technology and the Faculty of Civil Engineering at Technical University Vienna, aims to explore the use of sorptive materials based on clay minerals and green elements to stabilize indoor humidity levels, maintaining a range of 40–50% throughout

the day. The main aim is to identify materials capable of regulating the humidity in the range of 35–55% at typical indoor temperatures through their sorptive activity. A suitable material should have the steepest possible sorption curve in the 35–55% relative humidity region and the largest possible difference in moisture content between the limit states (sorption capacity), allowing it to absorb moisture at high relative humidity and release it at low relative humidity. This paper describes the initial phase of research work, where raw materials based on unfired ceramics were selected and evaluated. These materials will further be combined with active green components and conventional measures, such as ventilation and targeted air exchange, to improve indoor climate control.

2. Materials and Methods

Based on the knowledge obtained from previous research works, 5 locally available clay types (further marked as A, B, C, D, and E) from the Czech Republic were selected for this study. The aim was to compare traditional clays with mixed clay minerals of different proportions (clays A and B below) to clays containing predominantly a single type of clay mineral (clays C, D, and E).

- Clay A was mainly based on kaolinite and illite, with an Al_2O_3 content of approximately 38% and a loss on ignition of 11%.
- Clay B also contained kaolinite and illite, though with a higher proportion of illite. It had 32% Al_2O_3 and an 8% loss on ignition.
- Clay C was mainly composed of kaolinite, with about 43% Al_2O_3 and a 15% loss on ignition.
- Clay D was montmorillonitic clay, containing roughly 20% Al_2O_3 and an 8% loss on ignition.
- Clay E was predominantly illitic clay, with an Al_2O_3 content of about 26% and a 16% loss on ignition.

The chemical composition of the different clay types is given in Table 1 below.

Table 1. Chemical composition of clays [%].

Type of Clay/ Chemical Compound	SiO_2	Al_2O_3	TiO_2	Fe_2O_3	CaO	MgO	K_2O	Na_2O
A	54.05	37.87	1.00	2.65	0.51	0.49	2.75	0.33
B	58.31	31.56	1.20	3.34	0.20	1.02	3.70	0.30
C	50.41	43.32	1.95	2.12	0.60	0.30	0.65	0.57
D	56.57	19.80	1.40	12.49	1.39	3.21	2.70	0.36
E	60.60	26.34	1.44	4.34	0.31	0.56	3.96	0.45

A sample of 5 selected clay types is shown in Figures 2 and 3.

Sample A

Sample B

Sample C

Figure 2. Photos of clay samples A, B, and C.

Sample D **Sample E**

Figure 3. Photos of clay samples D and E.

2.1. Laboratory Tests on Clay Materials

The test clay samples were subjected to microscopic analysis on a Keyence VHX-950F optical microscope (KEYENCE, Mechelen, Belgium) and then subjected to X-ray diffraction analysis on a PANalytical Empyrean (Malvern Panalytical Ltd., Malvern, UK). X-ray diffraction analysis is based on the diffraction of X-rays on the crystal lattice of the sample and is used to determine the mineralogical composition of substances. It is based on the combination of two principles: the crystallographic arrangement of substances and the interaction of X-ray radiation with particles forming the crystal lattice of substances. X-rays have a wavelength comparable to the distances between atoms in solids. If they hit the crystal, much of the radiation will pass through the crystal unhindered. However, a small part of the radiation is deflected (bent) by the crystal. This phenomenon is called X-ray diffraction. If a suitable detector is placed behind the crystal, the deflected beams will create characteristic patterns on it. The cause of diffraction is the scattering of X-rays on individual atoms of the crystal lattice. X-ray radiation is noticeably reflected only in those directions in which it interferes (wave folding). This condition is described by the Bragg equation

$$n \times \lambda = 2 \times d \times \sin\theta \quad (1)$$

where

d—distance between parallel grid planes [m]
λ—wavelength of X-rays [m]
θ—the angle between the X-ray beam and the grating plane [°]
n—a natural number that indicates the order of diffraction

The qualitative composition was mainly performed using the Rietveld method. Furthermore, particle size determination was performed using a Malvern Mastersizer laser granulometer (Malvern Panalytical Ltd., Malvern, UK). The individual devices are illustrated in Figure 4 below.

Optical microscopy **RTG-analyser** **Particle size analyzator**

Figure 4. Analytical measurements of clay test samples.

Another test on bulk clay samples was performed according to ASTM C837-09 [26]. This was the standard Test Method for Methylene Blue Index (MBI) of Clay, which can be used to quantitatively determine the clay content. In this test, the degree of plasticity $MBI = G_p$ is determined. G_p represents the volume of 0.01 molar solution of methylene blue in mL sorbed to 1 g of finely wiped sample.

$$MBI = G_p = \frac{V}{m} \quad (2)$$

where

V—volume of methylene blue solution at the equivalence point [mL]
m—sample weight [g]

An example of this test is shown in Figure 5 below.

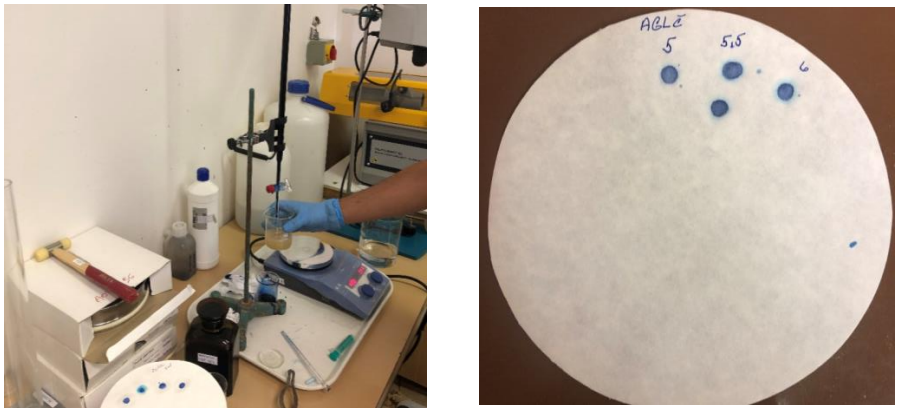

Figure 5. Determination of the Methylene Blue Index of Clay.

2.2. Laboratory Tests on Clay Materials—Plastic Dough

Key experiments were carried out on clay samples after mixing with water to form a plastic dough. Determination of optimum moisture content and sensitivity to drying was carried out.

The optimum moisture content of ceramic doughs was determined using a Pfefferkorn apparatus, following CSN 72 1074 [27]. The test involved deforming rollers of different moisture contents (40 mm high and 33 mm in diameter) by dropping a 1192 g plate from a height of 185 mm (see Figure 6). The ratio of the roller height before deformation, denoted by h_o, and after deformation, denoted by h_i, is referred to as the so-called deformation ratio d. The value of the optimum deformation ratio for the type of further processing envisaged was chosen to be $d = 0.6$.

(**a**) (**b**)

Figure 6. Determination of dough plasticity according to Pfefferkorn ((**a**) Pfefferkorn apparatus and (**b**) test roller).

The moisture content w was determined for each dough. The optimum amount of water w_{opt} for a particular clay recipe was then determined by calculation; see the following equations below:

$$w_{opt} = w_1 + \frac{w_2 - w_1}{d_2 - d_1} \times (d - d_1) \quad (3)$$

where

w_1—moisture content of the first (stiffer) sample [%]
w_2—moisture content of the second (more plastic) sample [%]
d_1—deformation ratio determined for the first (stiffer) specimen [−]
d_2—deformation ratio determined for the second (more plastic) specimen [−]
d = 0.6

In the next step, the susceptibility to drying was determined using the Bigot method, following CSN 721565-1 [28]. The measurements were performed on 100 × 50 × 20 mm samples that were made with optimum moisture content and were then dried successively while continuously recording the changes in dimensions and moisture content. Finally, the samples were dried at +110 °C to determine the critical moisture content w_{kb}.

The coefficient of sensitivity to drying, according to Bigot (*SDB*), was calculated using the following equation:

$$SDB = \frac{w_a - w_{kb}}{w_{kb}} \quad (4)$$

where

w_a—moisture content of the sample at the beginning of the measurement [%]
w_{kb}—critical moisture content [%]
SDB—sensitivity to drying according to Bigot [−]

2.3. Laboratory Tests on Hardened Clay Mat—Plastic Dough

From the individual clay formulations, test bodies were prepared for further testing of mechanical and sorption properties based on the evaluation of plastic dough properties.

For the determination of mechanical properties, beams with dimensions 20 × 20 × 120 mm were prepared from the plastic dough, dried at 105 °C, and stored in a desiccator. The determination of the flexural tensile strength was carried out according to CSN 72 1565-7 [29]. The flexural tensile strength σ_p [MPa] was determined according to the following relation below:

$$\sigma_p = \frac{3 \times F \times l}{2 \times b \times h^2} \quad (5)$$

where

b—section width [mm]
h—section height [mm]
F—maximum load, when deformed [N]
l—distance of supports [mm]

The compressive strength was measured on specimens following the flexural tensile strength test, with each specimen placed between two rigid, parallel steel plates of known area. The compressive strength, σ_{pd} [MPa], was then calculated using the following formula [30]:

$$\sigma_{pd} = \frac{F_{max}}{S} \quad (6)$$

where

F_{max}—maximum load [N]
S—pushing surface [mm^2]

An example of the mechanical properties testing process on clay beams is shown in Figure 7.

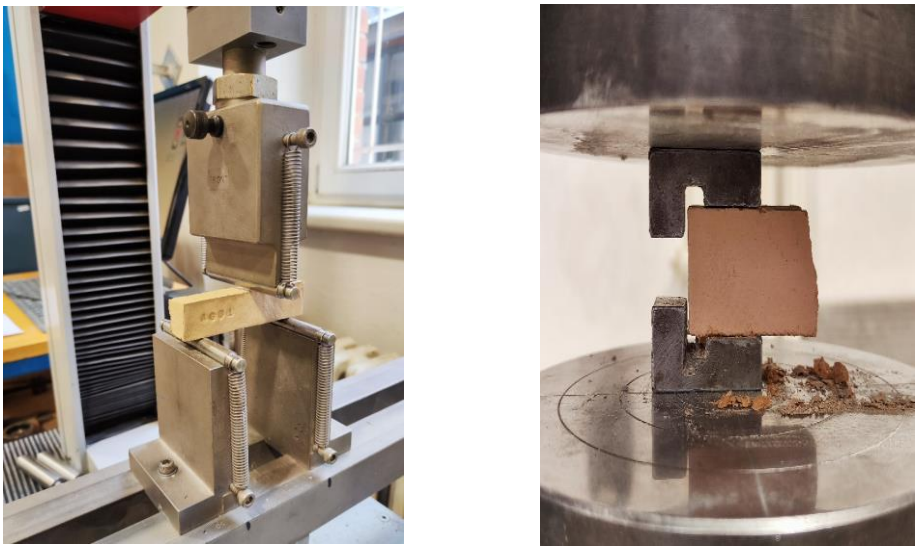

Figure 7. Determination of the mechanical properties.

The determination of sorption properties was carried out according to EN ISO 12571 "Hygrothermal performance of building materials and products—Determination of hygroscopic sorption properties" [31] on small samples weighing from 6 to 20 g. This involved the determination of equilibrium sorption and desorption isotherms at a temperature of 23 °C at different ambient humidities: 33, 53, 75, 85, and 98% RH.

Sorption and desorption curves were constructed for each set based on the mass changes in the test samples after reaching equilibrium moisture content, either from a dry or saturated state, under specified temperature and humidity conditions. Furthermore, testing of moisture buffering capacity according to DIN 18947 earth plasters requirements, testing, and labeling [32] was performed. The test procedure was slightly modified to meet the specific requirements of this research. Due to the nature of the clay samples, circular samples were produced with a thickness of 15 mm and a diameter of 17.8 cm; see Figure 8. The test specimens were first conditioned at 23 °C and 35% relative humidity in a climate chamber until the weight settled. Then, the relative humidity was increased to 65%, and the samples were weighed at precise intervals according to DIN 18947 [32].

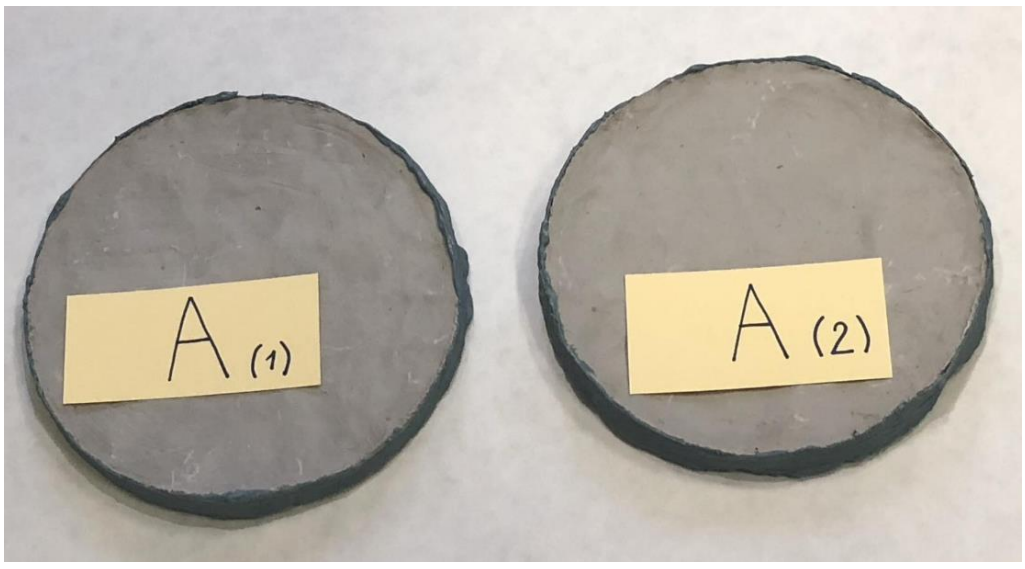

Figure 8. Sample test bodies for determination of moisture buffering capacity.

3. Results

As part of the laboratory tests on bulk clays, the mixtures of five clay samples A–E were imaged on a Keyence VHX-950F optical microscope (KEYENCE, Mechelen, Belgium). Due to the fact that clay particles tend to clump together, the test samples were ground in isopropyl alcohol solution. Graphical evaluation is shown in the following Figures 9–11, at 478× magnification. It can be said that despite the process of dispersing the clays with the C_3H_8O alcohol solution, the particles tend to clump together.

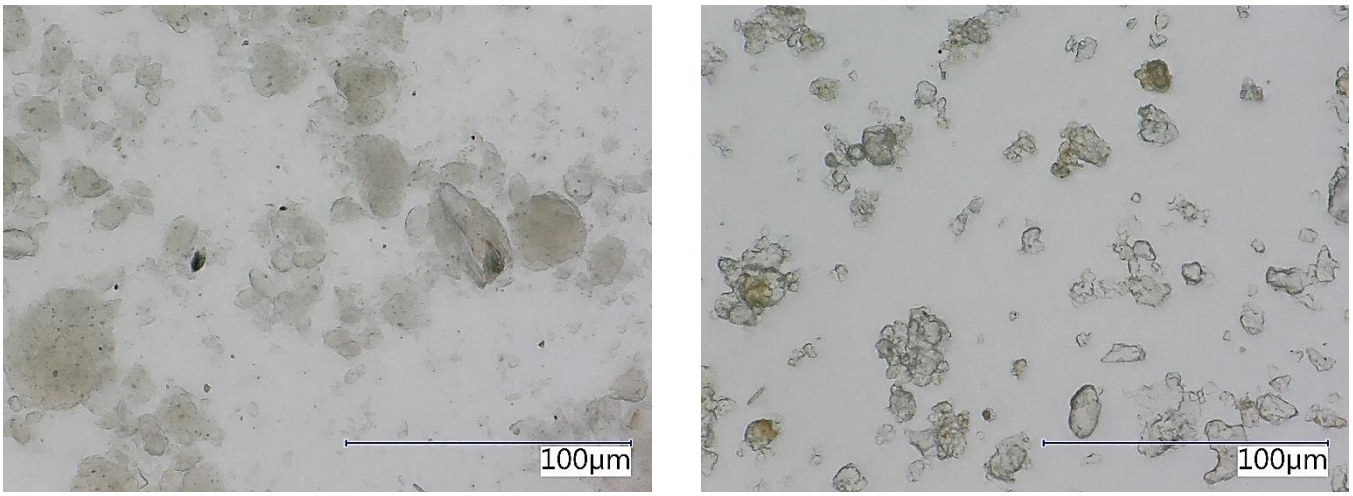

Sample A **Sample B**

Figure 9. Optical microscope image—magnification 478×.

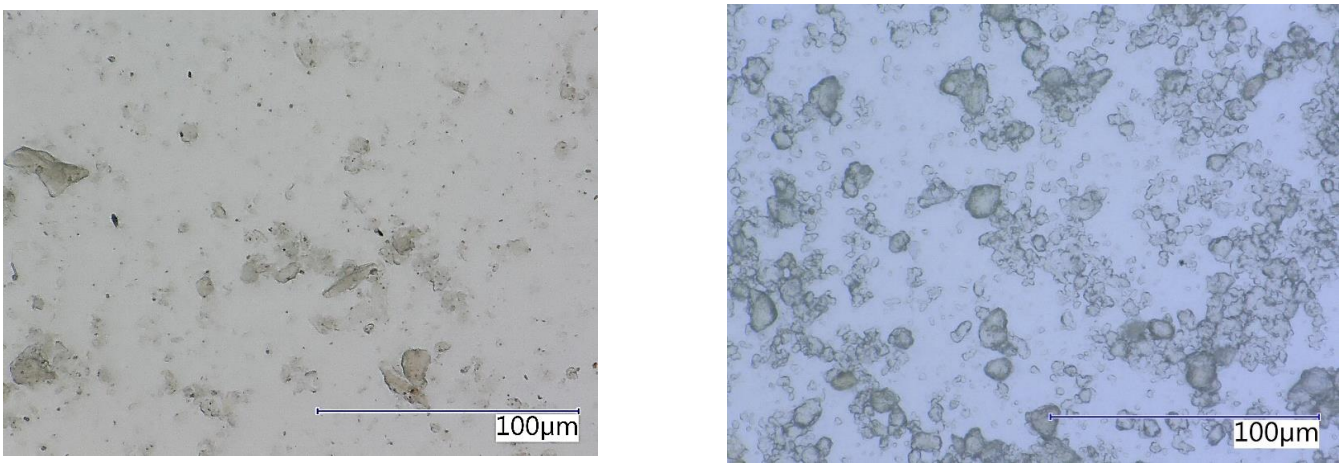

Sample C **Sample D**

Figure 10. Optical microscope image—magnification 478×.

Next, the samples underwent X-ray diffraction analysis using a PANalytical Empyrean device (Malvern Panalytical Ltd., Malvern, UK). The evaluation was carried out according to the Bragg equation. Radiographs were made for individual clay samples, i.e., the dependence of the intensity of the diffracted X-ray rays (I/I0) on the angle of incidence of the radiation (2θ°) [30], see Figures 12–16. The results indicated that all clay samples contained kaolinite (K) and illite (I). Mixture A was primarily composed of kaolinite (K), illite (I), mica (M), and a small amount of quartz (Q). Mixture B also contained kaolinite (K) and illite (I), along with muscovite (M) and a higher quartz content than Mixture A. Mixture C included kaolinite (K), illite (I), muscovite (M), and quartz (Q). Mixture D was mainly montmorillonite (M), illite (I), kaolinite (K), and orthoclase (O). Finally, Mixture E

consisted of illite (I), kaolinite (K), montmorillonite (M), and quartz (Q). The X-ray analysis further showed that clay A had the highest kaolinite content, while clay B had the highest proportion of illite.

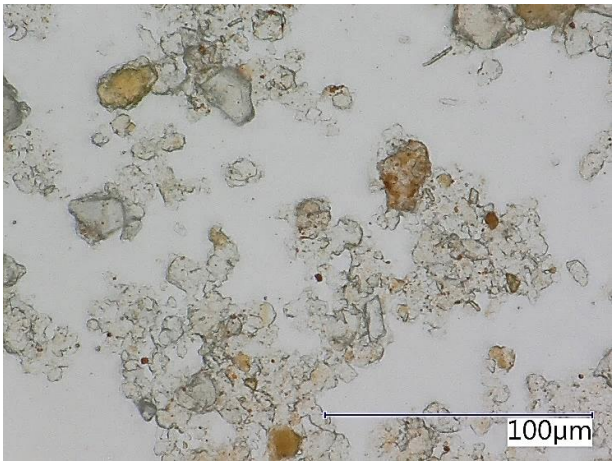

Sample E

Figure 11. Optical microscope image—magnification 478×.

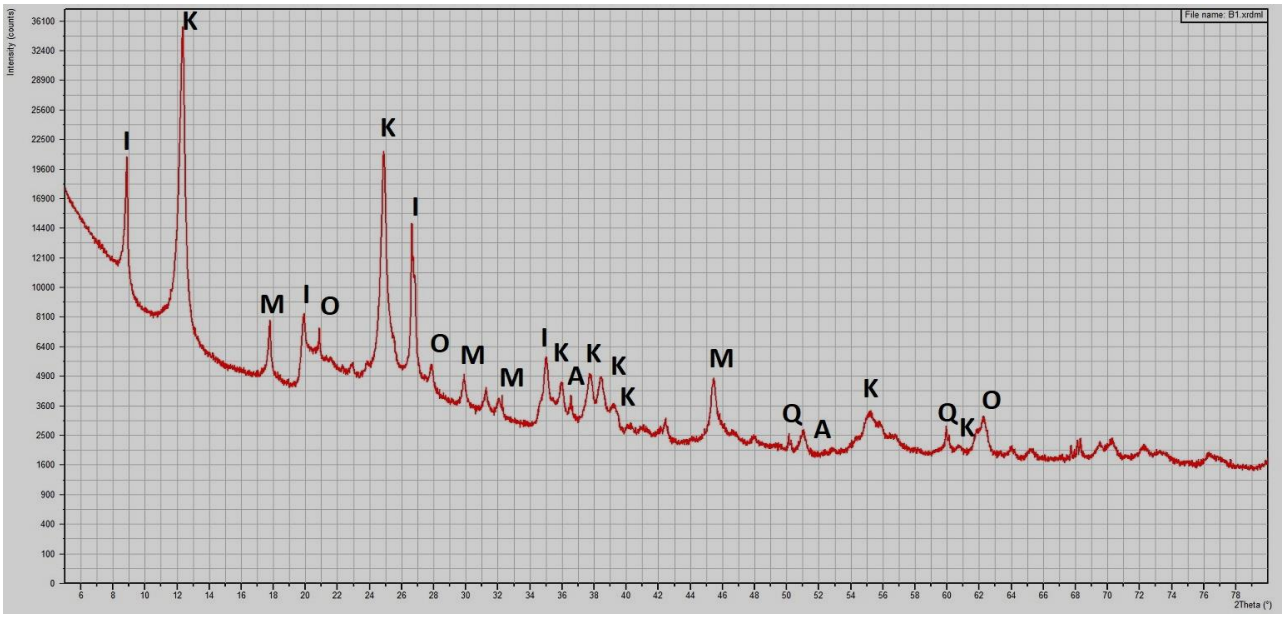

Figure 12. X-ray diffraction analysis—sample A (K—kaolinite, I—illite, M—mica, Q—quartz, O—orthoclase).

Particle size determination was performed using a laser granulometer, considering both wet and dry conditions of the clay samples. As shown in Figures 17 and 18, the clay particles tended to agglomerate into larger clusters, as also observed in the optical microscope images (see Figures 9–11). To address this, measurements were taken in both conditions. When dispersed in isopropyl alcohol (Figure 18), the clay particles separated effectively. The graphical analysis indicated that clay A had the finest particle size, with a mean size (d (0.5)) of 8.5 µm, while clay D, primarily composed of montmorillonite, had the largest particles, with a mean size of 25.3 µm. Clays C, B, and E exhibited intermediate mean particle sizes around 10.6 µm, consistent with observations from the optical microscope images.

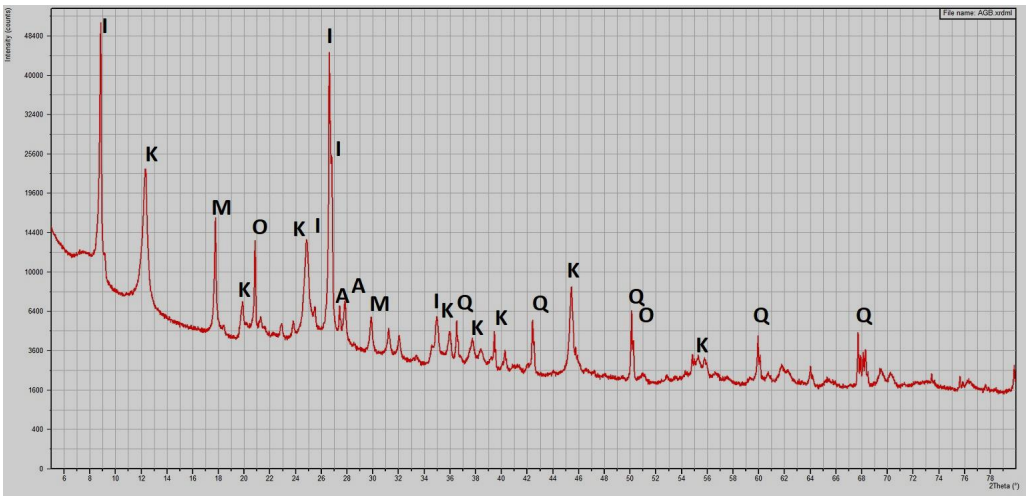

Figure 13. X-ray diffraction analysis—sample B (K—kaolinite, I—illite, M—muscovite, Q—quartz).

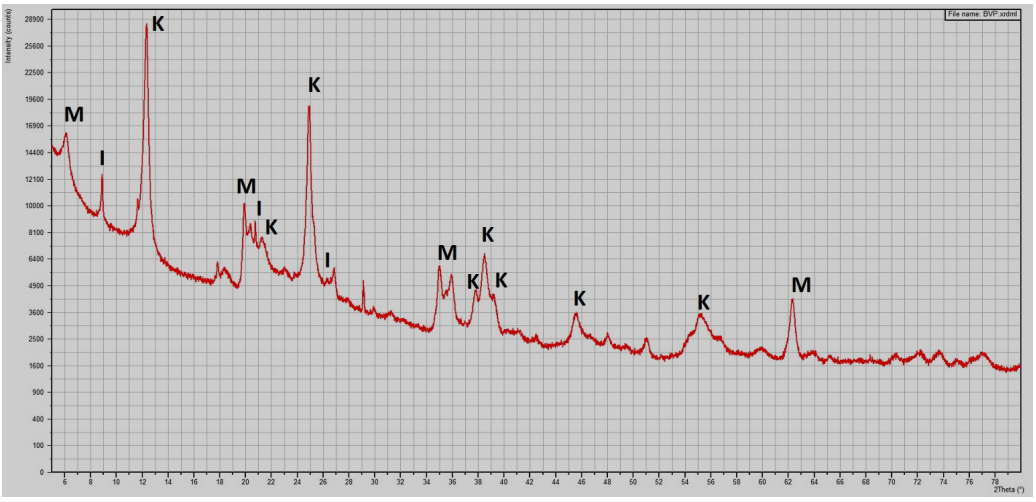

Figure 14. X-ray diffraction analysis—sample C (K—kaolinite, I—illite, M—muscovite).

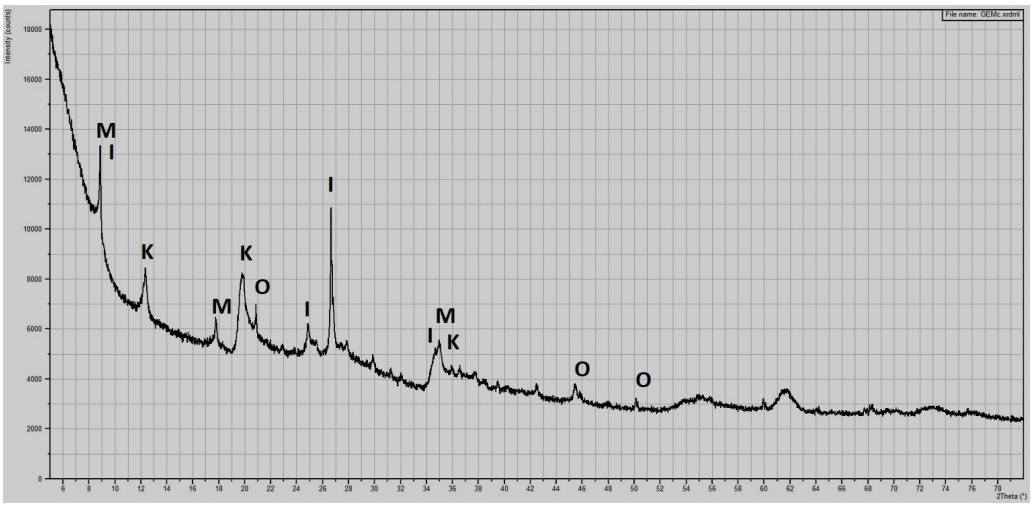

Figure 15. X-ray diffraction analysis—sample D (K—kaolinite, I—illite, M—muscovite, O—orthoclase).

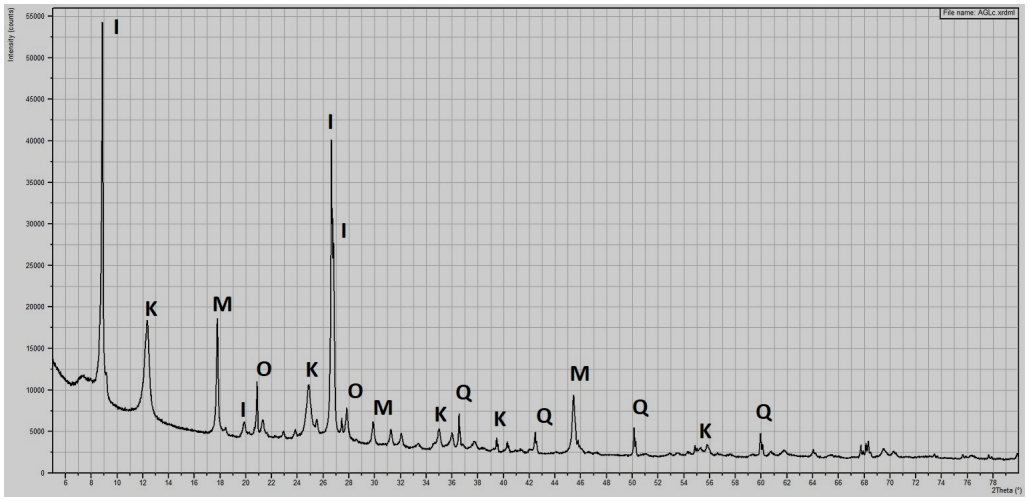

Figure 16. X-ray diffraction analysis—sample E (K—kaolinite, I—illite, M—muscovite, Q—quartz, O—orthoclase).

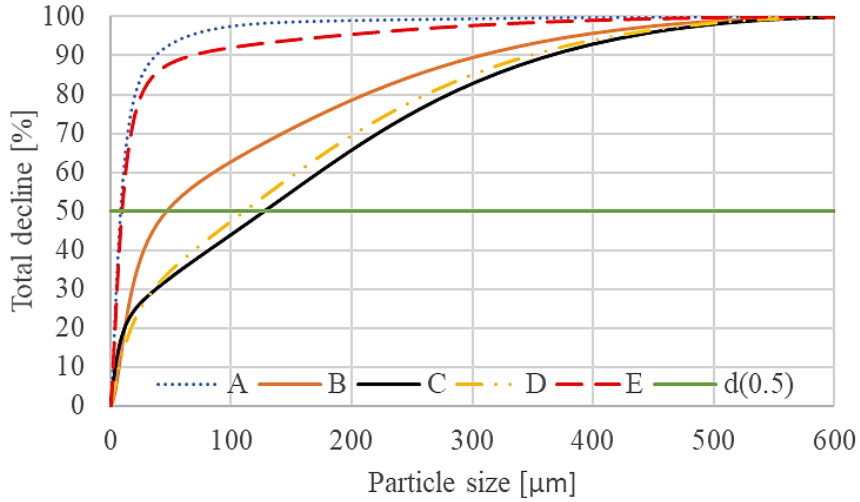

Figure 17. Sieve analysis—dry path.

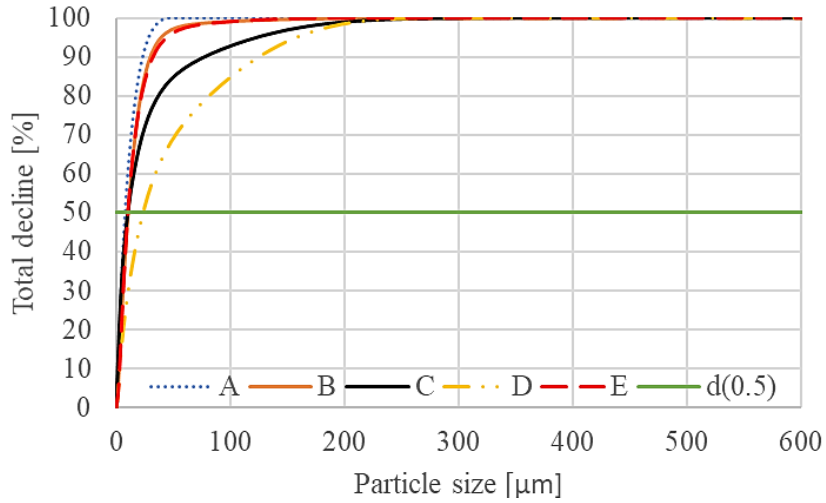

Figure 18. Sieve analysis—wet path—propane-2-ol.

The next test on the clay samples was the determination of the Methylene Blue Index (MBI). As shown in Table 2, mixtures A, B, C, and E were classified as moderately plastic according to ASTM C873-09 [26]. For mixture D, however, the methylene blue solution precipitated, preventing the determination of G_p.

Table 2. Evaluation of MBI of the mixtures of clays.

Mixture	Weight of Sample m [g]	Volume of Methylene Blue Solution [mL]	G_p [mL × g^{-1}]
A	1.1	5	5.55
B	1.1	7	6.36
C	1.1	6.5	5.91
D	1.1	5	*
E	1.1	5.5	5

* Precipitation—methylene blue dropped down to the test sample.

Laboratory tests were conducted to determine the optimum moisture content and drying sensitivity (SDB) of plastic doughs from all five clay mixtures. The results are summarized in Table 3. Notably, mixture D, composed primarily of montmorillonite, displayed a significantly higher moisture content and a correspondingly high CSB value, indicating a high sensitivity to drying. In contrast, mixtures B, C, and E showed low sensitivity to drying, while mixture A was classified as moderately sensitive.

Table 3. Evaluation of optimum moisture content and SDB for clay formulations.

Mixture	w_{opt} [w. %]	SDB [−]
A	35.93	1.07
B	27.15	0.95
C	32.67	0.86
D	50.58	2.89
E	28.65	0.94

Mechanical properties and sorption properties were determined on hardened test specimens of given dimensions.

The evaluation of the mechanical properties, specifically the flexural tensile strength and compressive strength, is shown in Figures 19 and 20. For flexural tensile strength, the highest average value was recorded for mixture A (1.94 MPa), while the lowest was for mixture C (0.3 MPa). In terms of compressive strength, mixture D had the highest average value (8.47 MPa), whereas mixture A reached 2.53 MPa.

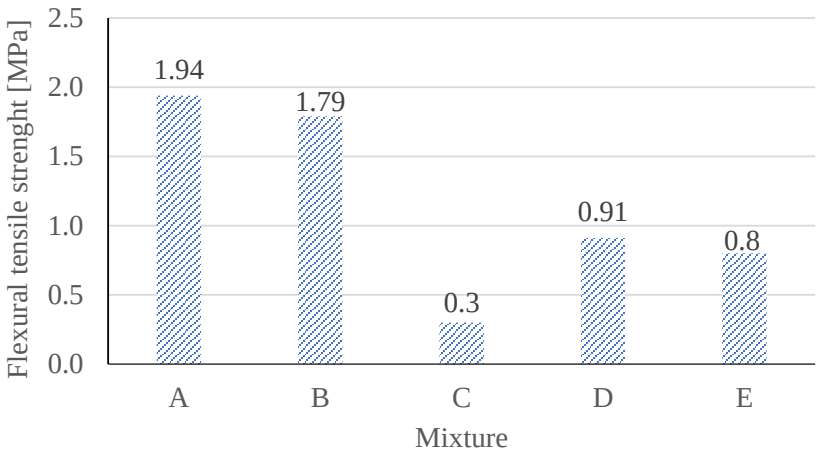

Figure 19. Overview of flexural tensile strength of clays.

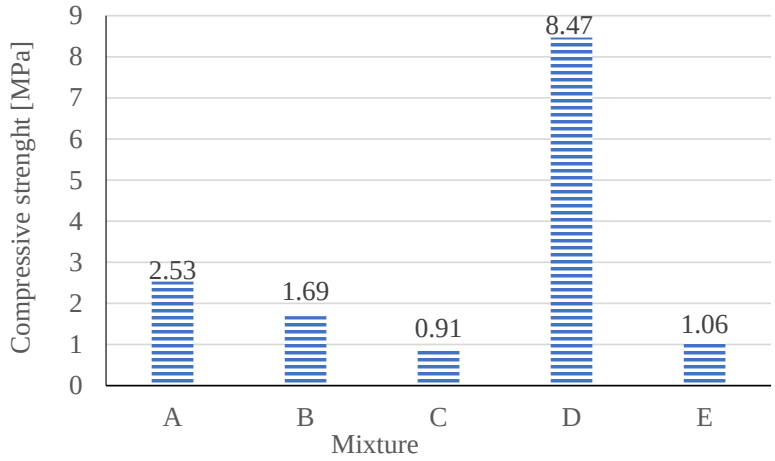

Figure 20. Overview of compressive strength of clays.

All five clay mixtures underwent testing to determine their sorption and desorption properties, with the resulting curves shown in Figures 21–25. The evaluation shows that mixture D, the montmorillonite-based clay, is the most humidity-sensitive, displaying the steepest curve in the 30–50% relative humidity range. However, a minor drawback of this clay type is its higher humidity hysteresis, which becomes noticeable only at high saturation or near complete dryness. This moisture sensitivity is attributed to the clay's structure (see Figure 1).

An assessment of the moisture buffering capacity is shown in Table 4 below. The samples were exposed to a change in relative humidity from 35 to 65% RH at +23 °C. Again, the highest moisture sensitivity was confirmed for mixture D and the lowest for mixture E. Mixture D adsorbed 167.6 g moisture per 1 m^2 in 12 h. On the other hand, the least moisture per 1 m^2 in 12 h was adsorbed by mixture E, 47.6 g.

Table 4. Evaluation of moisture buffering capacity [g/m^2].

Mixture	1 h	3 h	6 h	12 h
A	12.162	30.918	50.036	68.913
B	8.202	22.234	36.688	51.041
C	9.750	27.219	45.614	63.164
D	20.023	65.898	114.627	167.599
E	8.021	20.244	33.632	47.584

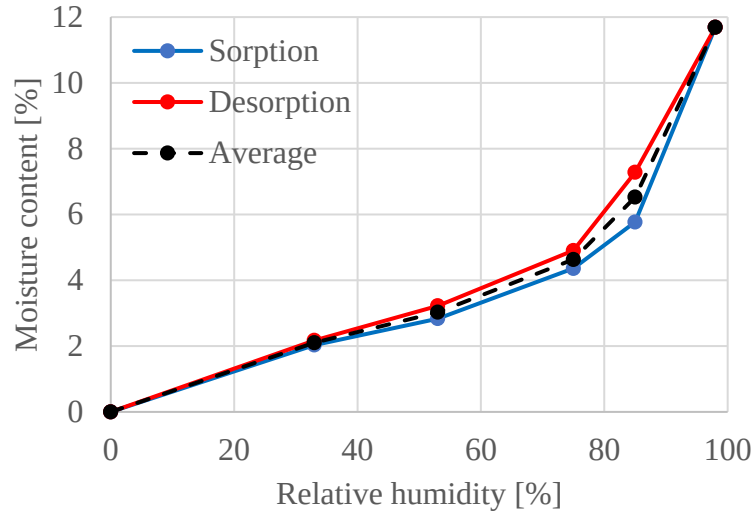

Figure 21. Sorption isotherm—clay A.

It is therefore evident that clay with a higher montmorillonite content is clearly the most sorption-sensitive and binds moisture significantly faster than other clay types.

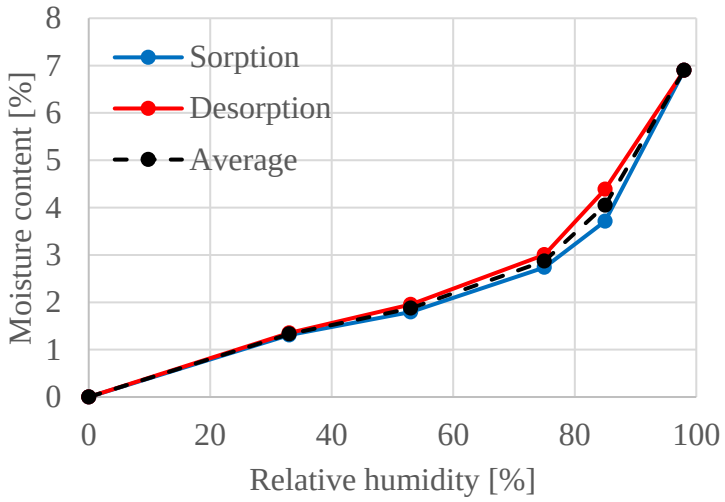

Figure 22. Sorption isotherm—clay B.

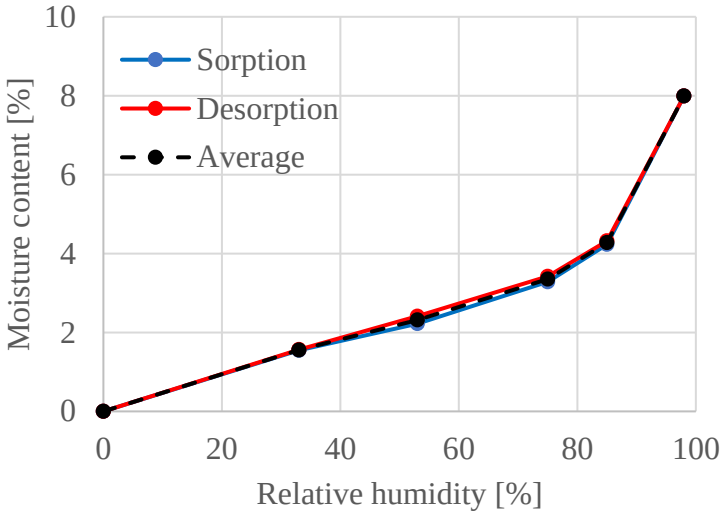

Figure 23. Sorption isotherm—clay C.

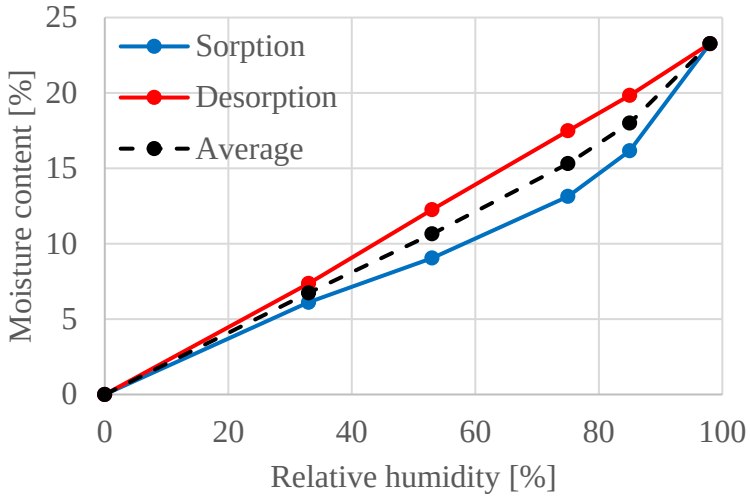

Figure 24. Sorption isotherm—clay D.

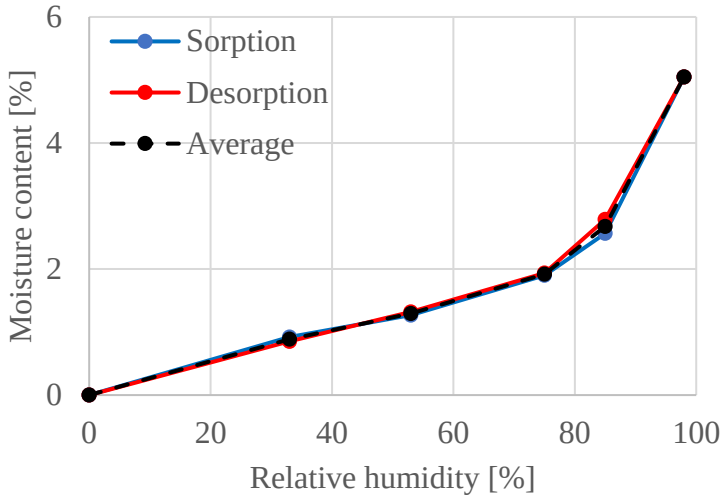

Figure 25. Sorption isotherm—clay E.

4. Discussion

In this research, five clays with distinct mineral compositions were selected to explore how mineralogy might influence the moisture behavior of sorptive elements prepared from them. Microscopic and X-ray diffraction analyses provided a detailed characterization of each formulation. Mixture A consisted mainly of kaolinite and illite, while mixture B also contained kaolinite and illite but with a higher proportion of illite. Mixture C was primarily composed of kaolinite, though in a lower overall proportion than mixture A. Mixture D was montmorillonite-based, and mixture E was primarily illite.

Evaluation of the optimum moisture content test revealed that the montmorillonite-based mixture, mixture D, required the highest water content for plastic dough formation at 50.58%. Conversely, mixtures with higher illite content required the least water, with mixture B at 27.15% and mixture E at 28.65%. This moisture requirement also correlated with drying sensitivity: mixture D exhibited a high CSB value of 2.89, indicating significant drying sensitivity. While expected, this behavior could limit practical applications, highlighting the need for further research on reducing drying sensitivity—possibly through natural fiber additives—while retaining favorable sorption properties. Mixtures B, C, and E showed low drying sensitivity, whereas mixture A, with a CSB > 1, was classified as moderately sensitive to drying.

Significant differences in mechanical properties were observed among the clay types. Mixture A showed the highest flexural tensile strength at 1.94 MPa, followed by mixture B at 1.79 MPa. Mixture D demonstrated the highest average compressive strength at 8.47 MPa, whereas mixture A recorded 2.53 MPa. In contrast, mixture C performed the worst in mechanical tests, with an average tensile strength of 0.3 MPa and compressive strength of 0.91 MPa. These results indicate that clay types differ considerably in both tensile and compressive strengths. Notably, tensile strength tests revealed some sensitivity to drying and microcrack formation, which may have slightly affected results. Overall, the montmorillonite-based mixture D exhibits highly favorable mechanical properties, making it the most promising for further applications.

Sorption characteristics confirmed that montmorillonite can bind a substantial amount of moisture within its structure. The montmorillonite-based mixture D showed significantly higher mass moisture content during sorption tests, with moisture levels ranging from 6.11% to 9.05% at relative humidities of 33% to 53% and from 7.36% to 12.26% during desorption (see Tables 5 and 6). On the contrary, mixture E retained the least moisture, with sorption values between 0.92% and 1.27% and desorption values from 0.85% to 1.32% within the same humidity range. These findings were further supported by moisture buffering capacity tests, where mixture D adsorbed approximately 167.6 g/m^2 of moisture over 12 h, compared to 47.6 g/m^2 for mixture E. According to the DIN 1894 standard,

clays D, A, and C can be classified in the adsorption class WC III (i.e., clays with excellent moisture adsorption). Since the adsorption rate was higher than 60 g/m^2 in 12 h, these parameters were achieved, for example, by Trambitski from Vilnius Gediminas Technical University [33].

Table 5. Evaluation of mass moisture content—sorption [g].

Mixture/Relative Humidity	A	B	C	D	E
33	2.03	1.31	1.55	6.11	0.92
53	2.83	1.80	2.22	9.05	1.27
75	4.36	2.74	3.28	13.13	1.90
85	5.77	3.71	4.23	16.16	2.56
98	11.69	6.90	7.99	23.27	5.05

Table 6. Evaluation of mass moisture content—desorption [g].

Mixture/Relative Humidity	A	B	C	D	E
33	2.17	1.35	1.57	7.36	0.85
53	3.22	1.95	2.41	12.26	1.32
75	4.90	3.00	3.42	17.49	1.94
85	7.28	4.39	4.32	19.83	2.79
98	11.69	6.90	7.99	23.27	5.05

In this case, however, the rate of moisture binding is key. As can be seen from the achieved values listed above, Figure 26 shows the course of moisture buffering in time.

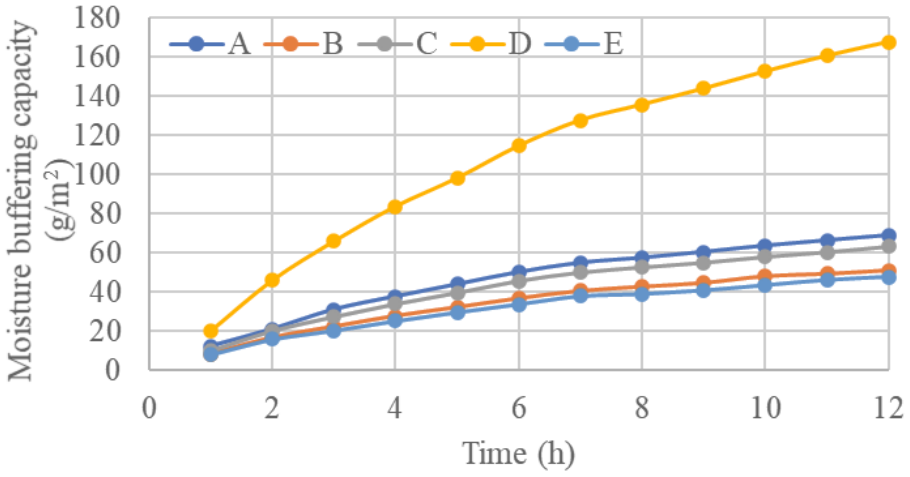

Figure 26. Dependence of moisture buffering capacity on time.

As can be seen, the humidity increase follows an approximately linear pattern for the first 7 h, after which the wetting rate begins to gradually decrease. This shift is influenced by factors such as the sample thickness and internal moisture redistribution. Based on this trend, the initial wetting rate, or moisture buffering rate, was determined with individual values displayed in Figure 27.

If we compare the obtained sorption characteristics with the moisture buffering capacity values obtained for a humidity change from 35% to 65%, it reveals that only partial moisture stabilization occurs within 12 h, and the observed capacity values are significantly lower than the theoretical values derived from recalculated sorption isotherms. For instance, Sample D, which demonstrated the highest activity, has a theoretical capacity of approximately 600 g/m^2 at stabilized humidity, but the actual sorption buffering capacity available for humidity control is around 28% of this value.

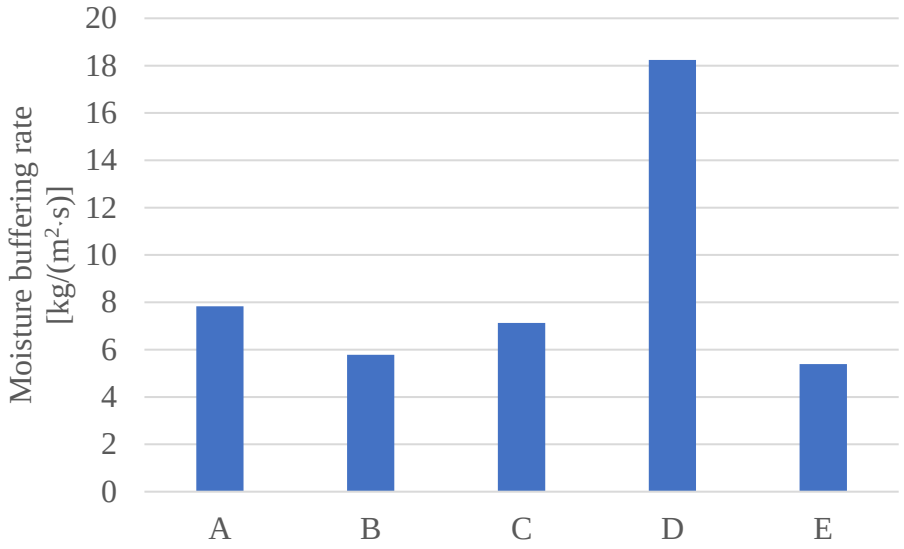

Figure 27. Moisture capacity rate of test samples.

Assuming a room with dimensions of 4 × 5 × 3 m and an interior temperature of 23 °C, we can derive key humidity characteristics. At this temperature, the partial pressure of saturated water vapor is $p_{d,sat}$ = 2807.8 Pa. For a relative humidity of 35%, the partial pressure of water vapor is p_d (35% RH) = 982.73 Pa, and for 65% RH, it is p_d (65% RH) = 1825.08 Pa, resulting in a difference of Δp_d = 842.34 Pa.

In this model, the difference in humidity for a 1 m^3 room is 6.16 g, which translates to a humidity change of 369.58 g for a 60 m^3 room when the relative humidity shifts from 35% to 65%. Thus, it can be assumed that using a tile from Sample D with a total area of approximately 2.2 m^2 would be sufficient to regulate this humidity. This indicates that applying the material to a smaller area of the wall, rather than covering the entire surface, could effectively manage indoor humidity levels.

5. Conclusions

The goal of this research work was to identify suitable raw materials for environmentally friendly sorption elements that can stabilize indoor environments under both high and low humidity conditions. In the future, these elements could complement frequently used green elements, such as green walls and plants, to help regulate indoor microclimates and thus ensure a healthier and more pleasant indoor environment for buildings.

As part of this research, five types of clays containing different mineral compositions—kaolinite, illite, and montmorillonite or their combinations—were subjected to laboratory tests to evaluate their behavior in moisture contact. Based on the results, especially the sorption characteristics and moisture buffering capacity, it can be concluded that using natural elements is a suitable ecological option for optimizing indoor microclimates. All five clay mixtures demonstrated the ability to effectively manage indoor humidity levels.

Notably, clays with a predominant montmorillonite content can effectively regulate humidity within the 35–65% range. These materials can utilize up to 27% of their total sorption capacity for humidity control over a 12 h period, making them sufficient for regulating indoor environments. Calculations indicate that a wall covering of approximately 2.2 m^2 would be adequate for effective humidity control in a room with a volume of 60 m^3.

However, based on evaluations of other tests, including mechanical properties and CBS, mixtures B and E appear most suitable for microclimate stabilization. Adding fibers containing cellulose and lignin, such as agricultural by-products like straw, flax, hemp, or wood, could further enhance their effectiveness.

Author Contributions: Conceptualization, J.P. and J.Z.; methodology, J.P., J.Z. and A.K.; formal analysis, J.P. and A.K.; investigation, J.P. and J.Z.; resources, J.P.; data curation, J.P., V.N., A.K., E.S. and A.S.; writing—original draft preparation, J.P., J.Z., A.K. and E.S.; writing—review and editing, J.P. and E.S.; visualization, J.P., V.N. and A.S.; supervision, J.P., A.K. and J.Z.; project administration, J.P. and A.K.; funding acquisition, J.P. and A.K. All authors have read and agreed to the published version of the manuscript.

Funding: This paper was elaborated with the financial support of the Czech Science Foundation (GACR), within the bilateral research project between the Czech Republic and Austria (project No. GF23-06542K) "Study of the hygroaccumulative effect of natural based materials and their influence on the moisture stability of the indoor environment of buildings" and project No. FAST-S-24-8528. Development and research of new types of composite materials cured with CO_2.

Data Availability Statement: The original contributions presented in the study are included in the article, further inquiries can be directed to the corresponding author.

Conflicts of Interest: The authors declare no conflicts of interest.

References

1. *EN 15665*; Ventilation for Buildings—Determining Performance Criteria for Residential Ventilation Systems. British Standards Institution: London, UK, 2009.
2. *EN 16798-1*; Energy Performance of Buildings—Ventilation for Buildings—Part 1: Indoor Environmental Input Parameters for Design and Assessment of Energy Performance of Buildings Addressing Indoor Air Quality, Thermal Environment, Lighting and Acoustics—Module M1-6. Asociacion Espanola de Normalizacion: Madrid, Spain, 2020.
3. Gentile, V.; Velasquez, J.D.V.; Fantucci, S.; Autretto, G.; Gabrieli, R.; Gianchandani, P.K.; Armandi, M.; Baino, F. 3D-printed clay components with high surface area for passive indoor moisture buffering. *J. Build. Eng.* **2024**, *91*, 109631. [CrossRef]
4. Peuhkuri, R.; Lone, H.; Time, B.; Gustavsen, A.; Ojanen, T.; Ahonen, K.J.; Harderup, L.-E.; Arfvidsson, J. *Moisture Buffering of Building Materials*; Rode, C., Ed.; Technical University of Denmark DTU: Copenhagen, Denmark, 2006.
5. Mishra, A.K.; Loomans, M.G.L.C.; Hensen, J.L.M. Thermal comfort of heterogenous and dynamic indoor conditions-An overview. *Build. Environ.* **2016**, *109*, 82–100. [CrossRef]
6. Taleghani, M.; Tenpierik, M.; Kurvers, S.; Dobbelsteen, A. A review into thermal comfort in buildings. *Renew. Sustain. Energy Rev.* **2013**, *26*, 201–215. [CrossRef]
7. *EN ISO 7730*; Ergonomics of the Thermal Environment—Analytical Determination and Interpretation of Thermal Comfort Using Calculation of the PMV and PPD Indices and Local Thermal Comfort Criteria. Czech Office for Standards, Metrology and Testing: Prague, Czech Republic, 2006.
8. McGregor, F.; Heath, A.; Shea, A.; Lawrence, M. The moisture buffering capacity of unfired clay masonry. *Build. Environ.* **2014**, *82*, 599–607. [CrossRef]
9. Yao, S.; Yan, Z.; Xu, B.; Bi, W.; Zhang, J.; Li, H.; Qu, J. The influence of different clay/sand ratios on the hygrothermal properties of earthen plasters in the Maijishan Grottoes. *Herit. Sci.* **2024**, *12*, 28. [CrossRef]
10. Emiroğlu, M.; Yalama, A.; Erdoğdu, Y. Performance of ready-mixed clay plasters produced with different clay/sand ratios. *Appl. Clay. Sci.* **2015**, *115*, 221–229. [CrossRef]
11. Palumbo, M.; McGregor, F.; Heath, A.; Walker, P. The influence of two crop by-products on the hygrothermal properties of earth plasters. *Build. Environ.* **2016**, *105*, 245–252. [CrossRef]
12. Samonin, V.V.; Podvyaznikov, M.L.; Spiridonova, E.A.; Khrylova, E.D.; Khokhlachev, S.P.; Garabadzhiu, A.V. Production of Composite Sorption-Active Materials Based on Carbon Black and Clay Material from Man-Made Waste. *Russ. J. Gen. Chem.* **2023**, *93*, 715–722. [CrossRef]
13. Deliniere, R.; Aubert, J.E.; Rojat, F.; Gasc-Barbier, M. Physical, mineralogical and mechanical characterization of ready-mixed clay plaster. *Build. Environ.* **2014**, *80*, 11–17. [CrossRef]
14. Darling, E.K.; Cros, C.J.; Wargocki, P.; Kolarik, J.; Morrison, G.C.; Corsi, R.L. Impacts of a clay plaster on indoor air quality assessed using chemical and sensory measurements. *Build. Environ.* **2012**, *57*, 370–376. [CrossRef]
15. Maddison, M.; Mauring, T.; Kirsimäe, K.; Mander, Ü. The humidity buffer capacity of clay–sand plaster filled with phytomass from treatment wetlands. *Build. Environ.* **2009**, *44*, 1864–1868. [CrossRef]
16. Liuzzi, S.; Hall, M.R.; Stefanizzi, P.; Casey, S.P. Hygrothermal behaviour and relative humidity buffering of unfired and hydrated lime-stabilised clay composites in a Mediterranean climate. *Build. Environ.* **2013**, *61*, 82–92. [CrossRef]
17. Zhou, Y.; Trabelsi, A.; Mankibi, M.E. Hygrothermal properties of insulation materials from rice straw and natural binders for buildings. *Constr. Build. Mater.* **2023**, *372*, 130770. [CrossRef]
18. Abbas, M.S.; McGregor, F.; Fabbri, A.; Ferroukhi, M.Y.; Perlot, C. Effect of moisture content on hygrothermal properties: Comparison between pith and hemp shiv composites and other construction materials. *Constr. Build. Mater.* **2022**, *340*, 2–15. [CrossRef]

19. Gentile, V.; Libralato, M.; Fantucci, S.; Shtrepi, L.; Autretto, G. Enhancement of the hygroscopic and acoustic properties of indoor plasters with a Super Adsorbent Calcium Alginate BioPolymer. *J. Build. Eng.* **2023**, *76*, 107147. [CrossRef]
20. Mazhoud, B.; Collet, F.; Prétot, S.; Lanos, C. Effect of hemp content and clay stabilization on hygric and thermal properties of hemp-clay composites. *Constr. Build. Mater.* **2021**, *300*, 123878. [CrossRef]
21. He, Y.; Guo, S.; Zuo, X.; Tian, M.; Zhang, X.; Qu, L.; Miao, J. Smart Green Cotton Textile with hierarchically responsive conductive network for personal healthcare and thermal management. *ACS Appl. Mater. Interfaces* **2024**, *16*, 59358–59369. [CrossRef] [PubMed]
22. He, Y.; Guo, S.; Zhang, X.; Qu, L.; Fan, T.; Miao, J. Ultrathin two-dimensional membranes by assembling graphene and MXene nanosheets for high-performance precise separation. *J. Mater. Chem. A* **2024**, *12*, 30121–30168. [CrossRef]
23. Minke, G. *Earth Construction Handbook. The Building Material Earth in Modern Architecture*; WIT Press: Southampton, UK, 2000; p. 206.
24. Altmäe, E.; Ruus, A.; Raamets, J.; Tungel, E. Determination of Clay-Sand Plaster Hygrothermal Performance: Influence of Different Types of Clays on Sorption and Water Vapour Permeability. In Proceedings of the Cold Climate HVAC 2018 the 9th International Cold Climate Conference. Sustainable New Renovated Buildings in Cold Climates, Kiruna, Sweden, 12–15 March 2018. [CrossRef]
25. Lima, J.; Faria, P.; Silva, A.S. Earth Plasters: The Influence of Clay Mineralogy in the Plasters' Properties. *Int. J. Archit. Herit.* **2020**, *14*, 948–963. [CrossRef]
26. *ASTM C837-09*; Standard Test Method for Methylene Blue Index of Clay. ASTM International: West Conshohocken, PA, USA, 2019.
27. *CSN 72 1074*; Determination of Optimum and Processing Moisture of Ceramic Masses by Means of Pfefferkorn Apparatus. Czech Office for Standards Metrology and Testing: Prague, Czech Republic, 2015.
28. *CSN 721565-1*; Testing of brick clays. Determination of Moisture Content. Czech Office for Standards, Metrology and Testing: Prague, Czech Republic, 1986.
29. *CSN 72 1565-7*; Testing of Brick Clays. Determination of the Transverse Strength. Czech Office for Standards, Metrology and Testing: Prague, Czech Republic, 1986.
30. Sokolář, R.; Nevřivová, L.; Vodová, L.; Grygarová, S. *Refractory Clays in the Czech Republic and the Methodology for Assessing Their Properties*; Academic Publisher CERM: Brno, Czech Republic, 2012.
31. *EN ISO 12571*; Hygrothermal Performance of Building Materials and Products—Determination of Hygroscopic Sorption Properties. Czech Office for Standards, Metrology and Testing: Prague, Czech Republic, 2022.
32. *DIN 18947*; Earth Plasters—Requirements, Test and Labelling. German Institute for Standardization: Berlin, Germany, 2024.
33. Trambitski, Y. Research of Structure and Durability of Natural Polymer Modified Clays. Doctoral Dissertation, Vilnius Gediminas Technical University, Vilnius, Lithuania, 2024. [CrossRef]